Global Stabilization of Similar Formation via Edge-Based Clique Addition

Gen He, Gangshan Jing, Yongduan Song

School of Automation, Chongqing University, Chongqing 400044, China.

Abstract

In this paper, the focus is on distributed similar formation stabilization, which aims to design a distributed controller to stabilize a group of agents to a desired formation, allowing for arbitrary translations, rotations, and scaling. While existing literature has produced fruitful results in this area, current approaches often rely on restrictive conditions regarding the inter-agent interaction graph. This paper introduces a novel approach using a clique-based control law, along with the concept of "edge-based clique addition", which offers a more lenient graphical condition compared to previous clique-based methods. By concentrating on a single clique with the new controller, the paper establishes a necessary and sufficient condition for determining the clique shape uniquely, a novel contribution to the field. Furthermore, the paper proposes the graph construction method "edge-based clique addition", which ensures that the multi-agent system achieves global similar formation stabilization. Similar to distance-based formation control, the proposed controller only necessitates each agent to capture the relative positions from neighbors in its local coordinate frame, without the need for coordinate system alignment or wireless communications. Finally, a simulation example is provided to demonstrate the effectiveness of the proposed control strategy.

Key words: Multi-agent systems; distributed control; formation stabilization.

1 Introduction

Formation control of multi-agent system has wide-ranging applications in real-world scenarios, such as joint composition, exploration and rescue missions [1–3]. Achieving overall formation solely based on the local state information of neighbors is a topic of widespread interest. In the past studies, formation control methods based on different measurements have emerged [4], mainly classified into the following categories: displacement-based(relative position) [5–9], distance-based [10–14], bearing-based [15–19] and angle-based [20–22].

In displacement-based [6,7] and bearing-based [15–18] approaches, it is necessary to align the coordinate systems of each agent to ensure that the relative positions understood by each agent are the same. One solution is to achieve consensus on coordinate systems among agents through frequent information exchange [7,16,23], which is invalid in a communication-denied environment. On the other hand, distance and angle measurements are independent of coordinate frames, therefore have been extensively studied in [10–14] and [24,20,21,25,22], respectively. However, global convergence of formation control based on angle measurements remains to be a challenging problem.

In this paper, we focus on formation stabilization based on relative position measurements in individual local coordinate frames, without the need for coordinate alignment and wireless communication between agents.

Global convergence of formation control via local displacement measurements has been achieved through different approaches. In [26,27], the authors propose the complex Laplacian matrix approach for formations with leaders. In [28,29], the authors demonstrate the effectiveness of the affine formation control approach in achieving global convergence to a similar formation. In [25,30], global convergence for triangulated graphs is achieved by using linear angle constraints and local relative position

⋆ This work was supported in part by the National Key Research and Development Program of China under grant (No.2022YFB4701400/4701404), the National Natural Science Foundation of China under grant (62203073), and the Natural Science Foundation of Chongqing under Grant (CSTB2022NSCQ-MSX0577). Corresponding author: Gangshan Jing.

Email addresses: 202213021036@stu.cqu.edu.cn (Gen He), jinggangshan@cqu.edu.cn (Gangshan Jing), ydsong@cqu.edu.cn (Yongduan Song).

measurements in the absence of leaders. However, these approaches are not applicable to more general graphs.

All the aforementioned formation approaches require carefully designing the formation graph so that the constraints are consistent with the target formation shape and the graphical condition can be satisfied. In fact, a more flexible approach to encoding a formation shape as a graph is using cliques [31–33]. Moreover, the clique-based method is also based on purely relative position measurements in local coordinate frames and is able to provide global convergence. In [33], a clique-based approach is proposed to achieve global convergence of the target formation up to rotations and translations. However, formation scaling is not allowed and the agents in the intersection of two maxcliques [1] are required to not belong to any other maxcliques. In [31,32], the authors define the clique rigidity, and provide the relationship between clique rigidity and formation degrees of freedom. However, global convergence of the control strategy is only obtained for complete graphs. It is observed that the global stabilization of similar formations under more general graph structures is challenging.

To sum up, while fruitful results regarding formation stabilization based on local relative position measurements are reported in literature, none (to the authors' best knowledge) is available without requiring restrictive conditions on the inter-agent interaction graph. In this paper, we revisit the clique-based formation control problem and propose a relaxed sufficient graphical condition for global stabilization of a similar formation. By employing a gradient-like controller, which is similar to [31–33], we provide analytic expressions for the time-varying scaling and rotation factors. It is interestingly found that under such a controller, the stabilization of partial agents in a clique to a desired manifold is equivalent to the stabilization of the whole clique to its desired shape. The key principle is that the two constraints on rotation and scaling parameters ($\alpha_m = 0, k_m = 1$) can provide compensatory constraints on the equilibrium domain when two agents are not directly constrained. By virtue of this fact, we propose the *edge-based clique addition* approach, which always induces a graph that renders global convergence of the formation system.

The main contributions of this paper can be summarized as follows.

- We propose a clique-based distributed controller for similar formation control, and provide explicit analytic expressions for the scaling and rotation factors (Lemma 2), which induce higher degrees of freedom of the formation, compared to [33]. We also prove that our factor updating approach achieves the global minimum of the objective function given desired and actual formations.
- For a single clique, we establish a necessary and sufficient condition for the unique determination of the actual formation shape in the equilibrium domain (Lemma 7). Based on this condition, we develop a graph construction approach called edge-based clique addition.
- Under the graph constructed by edge-based clique addition and the proposed control strategy, we show global stabilization of the similar formation. Compared to [31] and [33], the graphical condition for global convergence is much milder. Moreover, the convergent formation scale is guaranteed to be not larger than its initial value.

The rest of this article is organized as follows. Section 2 gives notations and problem formulation. Section 3 introduces the control strategy, and the relationship between control inputs in local coordinate frames and the global coordinate frame. Section 4 analyzes the equilibrium domain of the control strategy and provides the edge-based clique addition approach for graph construction. Section 5 presents the stability analysis of the control strategy under the graph constructed by edge-based clique addition. Finally, section 6 provides the simulation results.

2 Preliminaries and problem formulation

2.1 Notations

Referring to [34,35], we give a series of definitions used in this paper. $\mathbb{R}^+$ represents the set of positive real numbers; $\mathbb{R}^n$ denotes the n dimensional Euclidean space; $\|\cdot\|$ is the Euclidean norm; $X^\top$ signifies the transpose of matrix X; I_n stands for the $n \times n$ identity matrix; For two matrices A and B, $A \otimes B$ represents the Kronecker product of the matrices. $\nabla_x f(x)$ denotes the gradient of the function $f(x)$ with respect to x; $R(\alpha) = \begin{bmatrix} \cos\alpha & -\sin\alpha \\ \sin\alpha & \cos\alpha \end{bmatrix}$ is the rotation matrix with respect to rotation angle $\alpha \in (-\pi, \pi]$; The superscript $\perp$ indicates a counter-clockwise rotation of a vector by $\pi/2$ in plane, i.e., $p^\perp = R(\frac{\pi}{2})p$ for $p \in \mathbb{R}^2$; The function $\text{atan2}(y, x)$ can be defined as follows:

$$\text{atan2}(y,x) = \begin{cases} 2\arctan(\frac{y}{\sqrt{x^2+y^2}+x}) & \text{if } x > 0, \\ 2\arctan(\frac{\sqrt{x^2+y^2}-x}{y}) & \text{if } x \le 0 \text{ and } y \neq 0, \\ \pi & \text{if } x < 0 \text{ and } y = 0, \\ \text{undefined} & \text{if } x = 0 \text{ and } y = 0. \end{cases}$$

An undirected graph, represented by $\mathcal{G} = (\mathcal{V}, \mathcal{E})$, contains a vertex set $\mathcal{V} = \{1, 2, ..., N\}$ and an edge set $\mathcal{E} = \{(i, j) \in \mathcal{E} : i, j \in \mathcal{V}\}$ with $(i, j) = (j, i)$; The set

[1] A maxclique is a clique that does not belong to any clique with more vertices.

of neighbors of vertex i is $\mathcal{N}_i = \{j \in \mathcal{V} : (i,j) \in \mathcal{E}\}$; Throughout this paper, all the considered graphs are undirected and time-invariant; Assigning a direction to each edge in an undirected graph is referred to as an orientation; The incident matrix can be represented by $H = [h_{ij}]$, whose the rows and columns are indexed by edges and vertices of $\mathcal{G}$ with an orientation. $h_{ij} = 1$ if vertex j is the head of ith edge, $h_{ij} = -1$ if vertex j is the tail of ith edge, and $h_{ij} = 0$ otherwise; A *clique* means a complete subgraph of graph $\mathcal{G}$, namely, any two vertices are adjacent in the clique; A *maxclique* C is a clique that does not belong to any clique with more vertices; Let $\mathcal{M}(\mathcal{G}) = \{1, ..., \bar{m}\}$ be the set of all the maxcliques in $\mathcal{G}$; The *r-intersection graph* of maxcliques of $\mathcal{G}$ is denoted by $\Upsilon_r(\mathcal{G}) = (\mathcal{M}(\mathcal{G}), \hat{\mathcal{E}}_r)$, where each edge $(i,j) \in \hat{\mathcal{E}}_r$ implies that maxcliques i and j have at least r vertices in common in $\mathcal{G}$. It can be observed that $\Upsilon_r(\mathcal{G})$ becomes sparser as r increases, i.e., $\hat{\mathcal{E}}_r \subseteq \hat{\mathcal{E}}_{r-1}$ for $r \geq 2$. We show the 2-intersection graph of maxcliques of $\mathcal{G}$ in Fig.1.

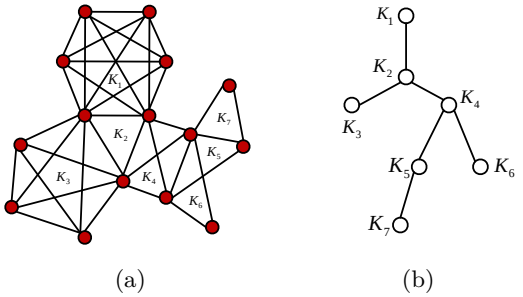

(a) (b)

Fig. 1. The example of 2-intersection graph of maxcliques in $\mathcal{G}$. (a) A formation graph $\mathcal{G}$ with 15 vertices and 7 maxcliques, which is also the desired formation of simulations. (b) the 2-intersection graph $\Upsilon_2(\mathcal{G}) = (\mathcal{M}(\mathcal{G}), \hat{\mathcal{E}})$. The vertices denote maxcliques and edges imply connected maxcliques have at least two common intersection.

2.2 Problem Formulation

Consider a group of N mobile agents in the plane with $p = [p_1^\top, p_2^\top, ..., p_N^\top]^\top \in \mathbb{R}^{2N}$, $p_i = [p_i^x, p_i^y]^\top \in \mathbb{R}^2$ is the position of agent $i \in \mathcal{V} = \{1, ..., N\}$. Each agent has a single-integrator dynamics:

$$\dot{p_i} = u_i, i \in \mathcal{V}, \tag{1}$$

where $u_i \in \mathbb{R}^2$ is the velocity input of agent i. In this paper, we will derive the control strategy based on gradient descent. It has been known that such controllers are applicable to not only single-integrator dynamics, but also more general dynamic systems, see [36].

Denote p_j^i as the position of agent j in the local coordinate frame of agent i. Each agent i can measure relative position from its neighbors in graph $\mathcal{G}$, i.e., $M_i = \{p_j^i - p_i^i, j \in \mathcal{N}_i\}$, here $\mathcal{N}_i$ is the neighbor set of agent i in $\mathcal{G}$. Note that the relative position information is measured by the onboard sensor of each agent, instead of communication (inter-agent information exchange).

The ultimate goal of the similar formation control problem considered in this paper is to drive the group of agents to stabilize a desired formation shape regardless of trivial motions including uniform translation, rotation, and scaling. Similar to [20,22], we use a framework $(\mathcal{G}, p^*)$ (where $\mathcal{G}$ is connected) to characterize the desired formation shape, where $p^* = [(p_1^*)^\top, (p_2^*)^\top, ..., (p_N^*)^\top]^\top \in \mathbb{R}^{2N}$, $p_i^* = [(p_i^*)^x, (p_i^*)^y]^\top \in \mathbb{R}^2$ is one realization of the target formation.

Problem 1: Given a configuration p^* forming the target formation shape, design a controller u_i based on M_i for each agent $i \in \mathcal{V}$, such that the stacked position states of agents, i.e., p, driven by (1), converges to a configuration of the following desired equilibrium set asymptotically:

$$\mathscr{S} = \{q \in \mathbb{R}^{2N} : q = k(I_N \otimes R)p^* + \mathbf{1}_N \otimes \xi, \\ k \in \mathbb{R}^+, R \in \mathrm{SO}(2), \xi \in \mathbb{R}^2\}. \tag{2}$$

The above-mentioned problem has been widely studied in literature via different approaches, e.g., distance-based [37,10], affine formation control [29,28], complex Laplacian [26], clique-based[33,32], angle-based [20,25]. Although [10,33] and [25] have all obtained global convergence, they often require restrictive graphical conditions. In this paper, we revisit Problem 1 and adopt the clique-based approach. Different from [33], we introduce a scaling parameter to achieve formation stabilization with higher degrees of freedom. Moreover, we will show that a graph constructed by edge-based clique addition suffices to ensure global convergence of our controller, which is a relaxed graphical condition.

3 Clique-Based Formation Control

In order to achieve distributed formation control, we encode the formation information through a set of inter-agent relative position vectors $M^* = \{p_j^* - p_i^*, i, j \in \mathcal{V}\}$, which is time-invariant and computed based on the target formation. Then the desired equilibrium set $\mathscr{S}$ can be transformed to

$$\mathscr{S} = \{q \in \mathbb{R}^{2N} : q_{ij} = kR(\alpha)p_{ij}^*, \forall\, i, j \in \mathcal{V}, \\ k \in \mathbb{R}^+, R(\alpha) \in \mathrm{SO}(2)\}, \tag{3}$$

where q_{ij} and p_{ij}^* are shorthands for $q_j - q_i$ and $p_j^* - p_i^*$, respectively.

It is natural to see that $p \in \mathscr{S}$ if and only if there exist $k \in \mathbb{R}^+$ and $R \in \mathrm{SO}(2)$ such that the following cost

equals zero:

$$\gamma = \sum_{i\in\mathcal{V}}\sum_{j\in\mathcal{V}} \left\|p_{ij} - kR(\alpha)p_{ij}^*\right\|^2, \tag{4}$$

where $p_{ij} = p_j - p_i$.

Directly designing the formation controller via the gradient of γ will require each agent to know the global coordinate frame information [7]. To address this issue, we adopt a clique-based method to achieve formation control. The underlying philosophy of a clique-based formation control approach is driving each maxclique to stabilize a desired pattern (which is a part of the desired formation) while coordinating different cliques via intersection agents. For any maxclique $m \in \mathcal{M}(\mathcal{G})$, we construct a cost function as follows:

$$\gamma_m = \frac{1}{4}\sum_{i\in\mathcal{I}_m}\sum_{j\in\mathcal{I}_m} \left\|p_{ij} - k_m R_m(\alpha_m)p_{ij}^*\right\|^2, \tag{5}$$

where $\mathcal{I}_m$ denotes the set of agents in the maxclique m, k_m is a non-negative scaling parameter, and $R_m(\alpha_m)$ is the rotation matrix associated with angle α_m. In the rest of the paper, we will use R_m as the shorthand of $R_m(\alpha_m)$ for symbol simplicity.

Compared with [33], adding a scaling parameter into the cost function of each maxclique induces an extra degree of freedom, i.e., formation scaling. With the introduction of the scaling parameter, the nonlinearity of the cost function increases, and the global stability analysis method in [33] becomes invalid. It can be observed that $\gamma_m = 0$ if and only if the actual clique m achieves the desired equilibrium.

Then we construct a new overall cost function as follows:

$$\hat{\gamma} = \sum_{m\in\mathcal{M}(\mathcal{G})} \gamma_m. \tag{6}$$

The newly designed overall cost function $\hat{\gamma}$ captures all the edges in $\mathcal{G}$ by encompassing all maxcliques. Then, we define the set of configurations that satisfy $\hat{\gamma} = 0$ as follows:

$$\begin{aligned} E^{\{\hat{\gamma}=0\}} = \{p \in \mathbb{R}^{2N} : \hat{\gamma} = 0, k_m \in \mathbb{R}^+, \\ R_m(\alpha_m) \in \mathrm{SO}(2), m \in \mathcal{M}(\mathcal{G})\}. \end{aligned} \tag{7}$$

To ensure that $E^{\{\hat{\gamma}=0\}}$ is able to describe the desired formation shape, we make the following assumption:

Assumption 1 *The 2-intersection graph $\Upsilon_2(G)$ is connected.*

The following lemma shows the equivalence between $\mathscr{S}$ and $E^{\{\hat{\gamma}=0\}}$ under Assumption 1.

Lemma 1 *$\mathscr{S} = E^{\{\hat{\gamma}=0\}}$ if and only if Assumption 1 holds.*

Proof. According to the definitions of $\mathscr{S}$ and $E^{\{\hat{\gamma}=0\}}$, we obtain $\mathscr{S} \subseteq E^{\{\hat{\gamma}=0\}}$ directly. Therefore, it suffices to show that $E^{\{\hat{\gamma}=0\}} \subseteq \mathscr{S}$ if and only if Assumption 1 holds. Next we prove sufficiency and necessity respectively.

Sufficiency. Consider an arbitrary configuration $p \in E^{\{\hat{\gamma}=0\}}$. Since $\Upsilon_2(\mathcal{G})$ is connected, without loss of generality, we can find two distinct maxcliques m_1 and m_2 such that they have at least two vertices i and j in common. Since $\hat{\gamma} = 0$, we have $p_{ij} = k_{m_1}R_{m_1}p_{ij}^* = k_{m_2}R_{m_2}p_{ij}^*$, implying that $R_{m_1} = R_{m_2}, k_{m_1} = k_{m_2}$. Recall that $\Upsilon_2(\mathcal{G})$ is connected, the equality can be trivially propagated throughout $|\mathcal{M}(\mathcal{G})|$ maxcliques, implying that there exist k and R such that $k_m = k$ and $R_m = R$, $\forall m \in \mathcal{M}(\mathcal{G})$, i.e., $p \in \mathscr{S}$.

Necessity. Assume Assumption 1 does not hold, then there are multiple connected components in $\Upsilon_2(\mathcal{G})$, and each pair of them have at most one vertex in common. According to the definitions of $\hat{\gamma}$ and γ_m, any two maxcliques m_1 and m_2 can have different k_m and R_m while ensuring $\gamma_{m_1} = \gamma_{m_2} = 0$ if they have at most one vertex in common. Therefore, $E^{\{\hat{\gamma}=0\}} \nsubseteq \mathscr{S}$ since $E^{\{\hat{\gamma}=0\}}$ contains configurations having different k_m and R_m for maxcliques in different connected components in $\Upsilon_2(\mathcal{G})$, which is a contradiction. The proof is completed. ■

Lemma 1 implies that the clique-wise cost function (5) has to be utilized on the premise of Assumption 1. Therefore, the formation control method proposed in this work always requires the validity of Assumption 1.

3.1 Control Strategy in the Global Frame

We aim to design a gradient descent control strategy for optimizing $\hat{\gamma}$. To this end, we compute its gradient as follows:

$$\begin{aligned} \nabla_{p_i}\hat{\gamma} &= \sum_{m\in\mathcal{M}(\mathcal{G})} \nabla_{p_i}\gamma_m \\ &= \sum_{m\in\mathcal{M}(\mathcal{G})} \left(\frac{\partial\gamma_m}{\partial\alpha_m}\frac{\partial\alpha_m}{\partial p_i} + \frac{\partial\gamma_m}{\partial k_m}\frac{\partial k_m}{\partial p_i} + \frac{\partial\gamma_m}{\partial p_i}\right), \end{aligned} \tag{8}$$

where the scaling parameter k_m and rotation parameter α_m are viewed as functions of p.

Given $p, p^* \in \mathbb{R}^{2N}$, next we design α_m and k_m such that

(i) the following equation holds:

$$\frac{\partial\gamma_m}{\partial\alpha_m} = \frac{\partial\gamma_m}{\partial k_m} = 0, \tag{9}$$

where $\alpha_m \in (-\pi, \pi]$ and $k_m > 0$;

(ii) the maxclique cost γ_m reaches its global minimum.

To ensure that α_m and k_m satisfy (i) and (ii) , we make the following assumption:

Assumption 2 *Denote* $\Delta'_m = \sum_{i\in\mathcal{I}_m}\sum_{j\in\mathcal{I}_m} p_{ij}^\top (p_{ij}^*)^\perp$, $\Delta_m = \sum_{i\in\mathcal{I}_m}\sum_{i\in\mathcal{I}_m} p_{ij}^\top p_{ij}^*$ *and set* $D = \{\Delta'_m = \Delta_m = 0\}$. *We assume* $p \notin D$ *during the formation process.*

Note that the set D is of measure zero, which implies that given a randomly generated configuration p, the probability of $p \in D$ is zero. Therefore, Assumption 2 is not restrictive, similar assumptions have been made in [31–33]. The following lemma gives the expressions of α_m and k_m under Assumption 2.

Lemma 2 *Given fixed* $p, p^* \in \mathbb{R}^{2N}$, *the following statements hold.*

(i). Equation (9) *holds if and only if*

$$\alpha_m = \operatorname{atan2}\left(\Delta'_{\mathrm{m}}, \Delta_{\mathrm{m}}\right), \tag{10}$$

and

$$k_m = \frac{\sum_{i\in\mathcal{I}_m}\sum_{j\in\mathcal{I}_m} p_{ij}^\top R_m p_{ij}^*}{\sum_{i\in\mathcal{I}_m}\sum_{j\in\mathcal{I}_m} (p_{ij}^*)^\top p_{ij}^*}, \tag{11}$$

(ii). The maxclique cost γ_m *reaches its global minimum if and only if* α_m *and* k_m *satisfy* (10) *and* (11), *respectively.*

Proof. (i). Restricting α_m to the region $(-\pi, \pi]$ and solving $\partial\gamma_m/\partial\alpha_m = 0$, we yield two possible solutions for α_m:

$$\alpha'_m = \operatorname{atan2}\left(\Delta'_m, \Delta_m\right), \quad \alpha''_m = \operatorname{atan2}\left(-\Delta'_m, -\Delta_m\right). \tag{12}$$

Similarly, solving $\partial\gamma_m/\partial k_m = 0$ gives a unique solution for k_m:

$$k_m = \frac{\sum_{i\in\mathcal{I}_m}\sum_{j\in\mathcal{I}_m} p_{ij}^\top R_m p_{ij}^*}{\sum_{i\in\mathcal{I}_m}\sum_{j\in\mathcal{I}_m} (p_{ij}^*)^\top p_{ij}^*}, \tag{13}$$

where

$$\sum_{i\in\mathcal{I}_m}\sum_{j\in\mathcal{I}_m} p_{ij}^\top R_m p_{ij}^* = \Delta_m \cos\alpha_m + \Delta'_m \sin\alpha_m. \tag{14}$$

According to (12), when $\alpha_m = \alpha'_m$, we have $\cos a_m = \frac{\Delta_m}{\sqrt{(\Delta'_m)^2+\Delta_m^2}}$ and $\sin a_m = \frac{\Delta'_m}{\sqrt{(\Delta'_m)^2+\Delta_m^2}}$, implying that $k_m > 0$. When $\alpha_m = \alpha''_m$, we have $\cos a_m = \frac{-\Delta_m}{\sqrt{(\Delta'_m)^2+\Delta_m^2}}$ and $\sin a_m = \frac{-\Delta'_m}{\sqrt{(\Delta'_m)^2+\Delta_m^2}}$, implying $k_m < 0$. We conclude that (9) is valid if and only if (10) and (11) hold, since k_m is constrained to be positive in (9).

(ii). Sufficiency. We prove the global optimality of γ_m by reduction to absurdity since it is complicated to obtain its Hessian matrix. Assume that there exists another pair $(R'_m, k'_m) \neq (R_m, k_m)$ globally minimizing γ_m. Next, we discuss the following three cases.

Case 1. $R_m \neq R'_m, k_m = k'_m$. According to (14), α_m in (10) results in

$$\frac{\partial\gamma_m^2}{\partial\alpha_m^2} = \frac{k_m}{2}(\Delta_m \cos\alpha_m + \Delta'_m \sin\alpha_m) > 0. \tag{15}$$

Thus α_m in (10) minimizes γ_m, which is a contradiction.

Case 2. $R_m = R'_m, k_m \neq k'_m$. Similar to Case 1, we have

$$\frac{\partial\gamma_m^2}{\partial k_m^2} = \frac{1}{2}\sum_{i\in\mathcal{I}_m}\sum_{j\in\mathcal{I}_m} \|p_{ij}^*\|^2 > 0, \tag{16}$$

implying that k_m in (11) minimizes γ_m, which is a contradiction.

Case 3. $R_m \neq R'_m, k_m \neq k'_m$. According to (10) and (11), the value of R_m is independent of k_m, thus we can select a new pair of parameter combination (R_m, k'_m). We can have the value of $\gamma_m(R_m, k'_m)$ less than $\gamma_m(R'_m, k'_m)$ based on case 2 and $\gamma_m(R_m, k_m)$ less than $\gamma_m(R_m, k'_m)$ based on case 1, i.e., $\gamma_m(R_m, k_m) < \gamma_m(R_m, k'_m) < \gamma_m(R'_m, k'_m)$. A contradiction arises.

In conclusion, γ_m obtains the global minimum if R_m and k_m satisfy (10) and (11), respectively.

Necessity. According to the necessary condition for stationary points of bivariate functions, the pair (R_m, k_m) satisfying (10) and (11) is the unique solution globally minimizing γ_m. ■

Recall the expression of $\nabla_{p_i}\hat{\gamma}$ in (8), based on $\partial\gamma_m/\partial\alpha_m = 0$ and $\partial\gamma_m/\partial k_m = 0$, we have

$$\nabla_{p_i}\gamma_m = \frac{\partial\gamma_m}{\partial p_i} = -\sum_{j\in\mathcal{I}_m}\left(p_{ij} - k_m R_m p_{ij}^*\right) \triangleq -u_{i_m}, \tag{17}$$

where u_{i_m} denotes the partial control input of agent i corresponding to maxclique m.

Then we can obtain the gradient descent controller of each agent i:

$$u_i = \sum_{m \in C_i} u_{i_m} = \sum_{m \in C_i} \left[\sum_{j \in \mathcal{I}_m} \left(p_{ij} - k_m R_m(\alpha_m) p_{ij}^* \right) \right], \tag{18}$$

where C_i is the set of all the maxcliques containing vertex i, k_m and $R_m(\alpha_m)$ are obtained by (10) and (11).

One can observe from the expression of u_i in (18) that each agent i only requires the information of $M_i^* = \{p_j^* - p_i^*, j \in \mathcal{N}_i\} \subseteq M^*$, which can be provided at the beginning of the formation process. During the formation process, each agent is not required to update M_i^* based on sensing or interactions with other agents. Moreover, the individual controller is distributed since it involves only relative information from neighbors. In Subsection 3.3, we will further show that the relative information that each agent requires can be computed in local coordinate frames.

3.2 Properties of the Control Law

We next examine some useful properties of the control law. Define the centroid and scale of the formation as

$$\bar{p} \triangleq \frac{1}{N} \sum_{i=1}^{N} p_i, \; s \triangleq \frac{1}{N} \sum_{i=1}^{N} \|p_i - \bar{p}\|^2, \tag{19}$$

respectively. We denote $p(0)$ as initial position of each agent and $s(0)$ as the initial scale with respect to $p(0)$. The following lemma shows the properties of $\bar{p}, p$ and s.

Lemma 3 *Under the controller* (18)*, the following statements hold for any* $t \geq 0$*.*

(i). The formation centroid $\bar{p}$ *is invariant.*

(ii). The positions of agents satisfy $\|p\| \leq \|p(0)\|$*.*

(iii). $s \leq s(0)$*.*

Proof. (i). Similar to [24], the invariance of the formation centroid $\bar{p}$ can be proved based on the symmetry of the graph.

(ii). The derivative of $\frac{1}{2}\|p\|^2$ can be expressed as follows:

$$\sum_{i=1}^{N} p_i^\top \dot{p}_i = \sum_{m \in \mathcal{M}(\mathcal{G})} \sum_{i \in \mathcal{I}_m} \left[p_i^\top \sum_{j \in \mathcal{I}_m} (p_{ij} - k_m R_m p_{ij}^*) \right]. \tag{20}$$

Note that

$$\begin{aligned} p_i^\top (p_{ij} - k_m R_m p_{ij}^*) + p_j^\top (p_{ji} - k_m R_m p_{ji}^*) \\ = - \|p_{ij}\|^2 + k_m p_{ij}^\top R_m p_{ij}^*. \end{aligned} \tag{21}$$

Then, equation (20) can be rewritten as

$$\begin{aligned} \sum_{i=1}^{N} p_i^\top \dot{p}_i &= \frac{1}{2} \sum_{m \in \mathcal{M}(\mathcal{G})} \sum_{i \in \mathcal{I}_m} \sum_{j \in \mathcal{I}_m} (- \|p_{ij}\|^2 + k_m p_{ij}^\top R_m p_{ij}^*) \\ &= \frac{1}{2} \sum_{m \in \mathcal{M}(\mathcal{G})} \left(-A + \frac{(\sum_{i \in \mathcal{I}_m} \sum_{j \in \mathcal{I}_m} p_{ij}^\top R_m p_{ij}^*)^2}{B} \right) \\ &\leq \frac{1}{2} \sum_{m \in \mathcal{M}(\mathcal{G})} \left(-A + \frac{C}{B} \right) \leq 0, \end{aligned} \tag{22}$$

where

$$A = \sum_{i \in \mathcal{I}_m} \sum_{j \in \mathcal{I}_m} \|p_{ij}\|^2,$$

$$B = \sum_{i \in \mathcal{I}_m} \sum_{j \in \mathcal{I}_m} \left\|p_{ij}^*\right\|^2,$$

$$C = (\sum_{i \in \mathcal{I}_m} \sum_{j \in \mathcal{I}_m} \|p_{ij}\| \left\|p_{ij}^*\right\|)^2,$$

and the inequality $C \leq A \cdot B$ can be obtained by the formula (2.3.4) in [38]. Therefore, the derivative of $\frac{1}{2}\|p\|^2$ is non-positive, implying $\|p\| \leq \|p(0)\|$.

(iii). We obtain the definitive of s as follows:

$$\dot{s} = \frac{2 \cdot \sum_{i=1}^{N} (p_i - \bar{p})^\top \dot{p}_i}{N}. \tag{23}$$

According to (i), (22) and

$$\sum_{i=1}^{N} \dot{p}_i = \sum_{i=1}^{N} u_i = 0,$$

we have $\dot{s} \leq 0$, implying $s \leq s(0)$. ■

The following lemma establishes the relationship between the controllers before and after rigid motions of the formation.

Lemma 4 *If the actual formation is transformed with uniform translations, rotations and scaling, i.e.,* $p'_{ij} = KR(\theta)p_{ij}, \forall i, j \in \mathcal{V}$*,* $K \in \mathbb{R}^+$ *and* $\theta \in (-\pi, \pi]$*, the new control input* u'_i *of each agent* i *satisfies*

$$u'_i = KR(\theta)u_i. \tag{24}$$

Proof. Without loss of generality, consider any maxclique $m, m \in \mathcal{M}(\mathcal{G})$, we can derive the new cost function of maxclique m as

$$\begin{aligned}\gamma'_m &= \frac{1}{4}\sum_{i\in\mathcal{I}_m}\sum_{j\in\mathcal{I}_m}\left\|p'_{ij}-k'_m R'_m p^*_{ij}\right\|^2 \\ &= \frac{K^2}{4}\sum_{i\in\mathcal{I}_m}\sum_{j\in\mathcal{I}_m}\left\|p_{ij}-\frac{k'_m}{K}R(\theta)^{-1}R'_m p^*_{ij}\right\|^2,\end{aligned} \tag{25}$$

where k'_m and R'_m are the new scaling and rotation factors to be designed.

Consider (5) and (25), (k_m, R_m) and $(k'_m/K, R^{-1}(\theta)R'_m)$ minimize γ_m and γ'_m, respectively. We can derive that $\frac{k'_m}{K}R^{-1}(\theta)R'_m = k_m R_m$, since there exists a unique solution that minimizes $\sum_{i\in\mathcal{I}_m}\sum_{j\in\mathcal{I}_m}\left\|p_{ij}-kRp^*_{ij}\right\|^2$, according to the necessity proof of (ii) of Lemma 2. Thus we have $k'_m = Kk_m, R'_m = R(\theta)R_m$ and obtain the relationship between u_i and u'_i as follows:

$$\begin{aligned}u'_i &= \sum_{m\in C_i}\sum_{j\in\mathcal{I}_m}\left(p'_{ij}-k'_m R'_m p^*_{ij}\right) \\ &= \sum_{m\in C_i}\sum_{j\in\mathcal{I}_m}\left(KR(\theta)p_{ij}-Kk_m R(\theta)R_m p^*_{ij}\right) \\ &= KR(\theta)u_i.\end{aligned} \tag{26}$$

The proof is completed. ■

3.3 Computation of the Control Inputs in the Local Frames

Next we will show the control input of each agent in its local coordinate frame, and the relationship between the control inputs obtained in the global coordinate frame and these obtained in local coordinate frames.

Define θ_i as the rotation angle between the local coordinate frame of each agent i and the global coordinate frame, where θ_i is unknown to each agent i. We use the superscript i to mark the quantities in the local coordinate system of agent i, therefore $p^i_{ij} = R(\theta_i)p_{ij}$. According to (5), the expression of the local cost function of agent i with respect to maxclique m is

$$\gamma^i_m = \frac{1}{4}\sum_{i\in\mathcal{I}_m}\sum_{j\in\mathcal{I}_m}\left\|p^i_{ij}-k^i_m R^i_m p^*_{ij}\right\|^2. \tag{27}$$

According to (5) and (27), agent i optimizes γ_m and γ^i_m separately through (R_m, k_m) and (R^i_m, k^i_m).

Similar to (18), the local control input of each agent is as follows:

$$u^i_i = \sum_{m\in C_i}\left[\sum_{k\in\mathcal{I}_m}\left(p^i_{ik}-k^i_m R^i_m(\alpha^i_m)p^*_{ik}\right)\right], \tag{28}$$

where the expressions of α^i_m and k^i_m are in (10) and (11), respectively, based on relative positions in local coordinate frames. According to Lemma 4, it holds that $k^i_m = k_m, R^i_m = R(\theta_i)R_m$ and

$$u^i_i = R(\theta_i)u_i, \tag{29}$$

since $p^i_{ij} = R(\theta_i)p_{ij}, \forall i, j \in \mathcal{I}_m$. The relationship between u^i_i and u_i characterizes the fact that agent i optimizes both γ^i_m and γ_m simultaneously. Thus we will analyze our controller in the global coordinate frame in the rest of the paper.

Based on the above analysis, we have the following result directly.

Lemma 5 *For any two vertices a and b in the maxclique m, R^a_m and R^b_m satisfy $(R(\theta_a))^{-1}R^a_m = (R(\theta_b))^{-1}R^b_m$.*

4 Equilibrium Analysis and Edge-Based Clique Addition

In this section, we will establish the relationship between the equilibrium set and the target formation shape. A formation graph construction approach will be proposed under which the equilibrium always corresponds to the target formation shape.

4.1 Equilibrium Analysis for Maxcliques

Denote

$$E^{\{u_i=0\}} = \{p \in \mathbb{R}^{2N} : u_i = 0, i \in \mathcal{V}\} \tag{30}$$

as the equilibrium set of the MAS with controller u_i defined in (18), we aim to find out the relationship between $E^{\{u_i=0\}}$ and $\mathscr{S}$. We first consider the case when graph $\mathcal{G}$ is completed, i.e., it only has one maxclique, which is itself. In this case, the following lemma shows that any equilibrium configuration always corresponds to the desired formation shape.

Lemma 6 *$E^{\{u_i=0\}} = \mathscr{S}$ if $\mathcal{G}$ is complete.*

Proof. Firstly, we prove that $E^{\{u_i=0\}} \subseteq \mathscr{S}$. Suppose $p \in E^{\{u_i=0\}}$. According to (18), for any two vertices $l_1, l_2 \in \mathcal{V}$, we have

$$\sum_{j\in\mathcal{V}}(p_{l_1 j}-kRp^*_{l_1 j}) = 0, \sum_{j\in\mathcal{V}}(p_{l_2 j}-kRp^*_{l_2 j}) = 0. \tag{31}$$

Subtracting the two equations, we have $p_{l_1 l_2} = kRp^*_{l_1 l_2}$. Therefore, $p \in \mathscr{S}$.

Next, we prove that $\mathscr{S} \subseteq E^{\{u_i=0\}}$. Consider the expression of $\mathscr{S}$ in (3), it is observed $\left\|p_{ij} - kRp^*_{ij}\right\|^2 = 0,\ \forall i,j \in \mathcal{V}$ under complete graph. Therefore, we can derive $u_i = \sum_{j\in\mathcal{V}} \left(p_{ij} - kRp^*_{ij}\right) = 0, i \in \mathcal{V}$. The proof is completed. ■

Remark 1 *Lemma 6 implies that given a maxclique m, $\{u_{i_m} = 0, i \in \mathcal{I}_m\}$ always corresponds to the desired formation for this maxclique. However, for a general graph consisting of multiple maxcliques, there always exist agents in the intersection of different maxcliques, whose equilibrium is more complicated to analyze. For example, let i be an agent lying in maxcliques $m_1, ..., m_s$. Then the equilibrium of agent i becomes $\{\sum_{j=1}^{s} u_{i_{m_j}} = 0\}$, which may not lead to $\{u_{i_{m_1}} = \cdots = u_{i_{m_s}} = 0\}$.*

For the sake of discussion, we define the agents lying in only one maxclique as *independent agents*. In fact, if the number of independent agents of a maxclique is sufficiently large, the equilibrium of this maxclique remains to fit the target formation. To show this, we consider any maxclique m with $|\mathcal{I}_m| \geq 3$, and let $\mathcal{I}_0$ ($\mathcal{I}_0 \subseteq \mathcal{I}_m$) be the set of independent agents in this maxclique.

Denote

$$E_m = \{p \in \mathbb{R}^{2|\mathcal{I}_m|} : u_{i_m} = 0, \\ k_m \in \mathbb{R}^+, R_m(\alpha_m) \in \mathrm{SO}(2), i \in \mathcal{I}_m\} \quad (32)$$

and

$$E_{m0} = \{p \in \mathbb{R}^{2|\mathcal{I}_m|} : u_{i_m} = 0, \\ k_m \in \mathbb{R}^+, R_m(\alpha_m) \in \mathrm{SO}(2), i \in \mathcal{I}_0\}. \quad (33)$$

The following lemma gives a necessary and sufficient condition on $|\mathcal{I}_0|$ for ensuring $E_m = E_{m0}$.

Lemma 7 *$E_m = E_{m0}$ if and only if $|\mathcal{I}_0| \geq |\mathcal{I}_m| - 2$.*

Proof. Without loss of generality, we focus on the case $k_m = 1$ and $R_m = I_2$. By the virtue of Lemma 4, the results can be extended to the case for $\forall k_m \in \mathbb{R}^+$ and $\forall R_m(\alpha_m) \in \mathrm{SO}(2)$.

It is observed that $E_m \subseteq E_{m0}$ since $\mathcal{I}_0 \subseteq \mathcal{I}_m$. Therefore, it suffices to show that $E_{m0} \subseteq E_m$ if and only if $|\mathcal{I}_0| \geq |\mathcal{I}_m| - 2$.

Before we enter into the main proof, we first analyze what kind of constraints on the configuration p that the set E_{m0} offers.

According to the expressions of k_m and R_m in (10) and (11), respectively, we have

$$\sum_{i\in\mathcal{I}_m}\sum_{j\in\mathcal{I}_m} p_{ij}^\top (p^*_{ij})^\perp = 0, \quad (34)$$

$$\sum_{i\in\mathcal{I}_m}\sum_{j\in\mathcal{I}_m} p_{ij}^\top p^*_{ij} = \sum_{i\in\mathcal{I}_m}\sum_{j\in\mathcal{I}_m} (p^*_{ij})^\top p^*_{ij}. \quad (35)$$

For ease of presentation, we define $p_{\mathcal{I}_m} = [p_1^\top, ..., p_{|\mathcal{I}_m|}^\top]^\top \in \mathbb{R}^{2|\mathcal{I}_m|}$ and $p^*_{\mathcal{I}_m} = [(p^*_1)^\top, ..., (p^*_{|\mathcal{I}_m|})^\top]^\top \in \mathbb{R}^{2|\mathcal{I}_m|}$. Consider (34), we have

$$\begin{aligned} &\sum_{i\in\mathcal{I}_m}\sum_{j\in\mathcal{I}_m} p_{ij}^\top (p^*_{ij})^\perp \quad (36)\\ &= 2\cdot [H_m \otimes I_2 \cdot p_{\mathcal{I}_m}]^\top \cdot I_{\frac{|\mathcal{I}_m|(|\mathcal{I}_m|-1)}{2}} \otimes W \cdot H_m \otimes I_2 \cdot p^*_{\mathcal{I}_m} \\ &= 2\cdot p_{\mathcal{I}_m}^\top H_m^\top H_m \otimes W \cdot p^*_{\mathcal{I}_m} \\ &= 2\cdot p_{\mathcal{I}_m}^\top L_m \otimes W \cdot p^*_{\mathcal{I}_m} \\ &= 2(p^*_{\mathcal{I}_m})^\top L_m \otimes W \cdot p_{\mathcal{I}_m} = 0, \end{aligned}$$

where $H_m \in \mathbb{R}^{\frac{|\mathcal{I}_m|(|\mathcal{I}_m|-1)}{2}\times|\mathcal{I}_m|}$ and $L_m \in \mathbb{R}^{|\mathcal{I}_m|\times|\mathcal{I}_m|}$ are the incidence matrix and Laplacian matrix, respectively, associated with the maxclique m, and $W = R(\frac{\pi}{2}) \cdot I_2$.

Meanwhile, we can obtain

$$\sum_{i\in\mathcal{I}_m}\sum_{j\in\mathcal{I}_m} (p^*_{ij})^\top (p^*_{ij})^\perp = 2(p^*_{\mathcal{I}_m})^\top L_m \otimes W \cdot p^*_{\mathcal{I}_m} = 0. \quad (37)$$

Subtract (37) from (36), yielding

$$\begin{aligned} &2(p^*_{\mathcal{I}_m})^\top L_m \otimes W \cdot p_{\mathcal{I}_m} - 2(p^*_{\mathcal{I}_m})^\top L_m \otimes W \cdot p^*_{\mathcal{I}_m} \quad (38)\\ &= 2(p^*_{\mathcal{I}_m})^\top L_m \otimes W \cdot q_{\mathcal{I}_m} = 0, \end{aligned}$$

where $q_{\mathcal{I}_m} = p_{\mathcal{I}_m} - p^*_{\mathcal{I}_m}$. Then consider (35), we have

$$\begin{aligned} &\sum_{i\in\mathcal{I}_m}\sum_{j\in\mathcal{I}_m} p_{ij}^\top p^*_{ij} - \sum_{i\in\mathcal{I}_m}\sum_{j\in\mathcal{I}_m} (p^*_{ij})^\top p^*_{ij} \quad (39)\\ =&2\cdot [H_m \otimes I_2 \cdot p_{\mathcal{I}_m}]^\top \cdot H_m \otimes I_2 \cdot p^*_{\mathcal{I}_m} - \\ &2\cdot [H_m \otimes I_2 \cdot p^*_{\mathcal{I}_m}]^\top \cdot H_m \otimes I_2 \cdot p^*_{\mathcal{I}_m} \\ =&2q_{I_m}^\top L_m \otimes I_2 \cdot p^*_{\mathcal{I}_m} = 2(p^*_{\mathcal{I}_m})^\top L_m \otimes I_2 \cdot q_{\mathcal{I}_m} = 0. \end{aligned}$$

When $k_m = 1$ and $R_m = I_2$, examine E_{m0} results in

$$u_{i_m} = \sum_{k\in\mathcal{I}_m} (p_{ik} - p^*_{ik}) = 0, i \in \mathcal{I}_0. \quad (40)$$

On the other hand, assume

$$u_{i_m} = \sum_{k\in\mathcal{I}_m} (p_{ik} - p^*_{ik}) = [x'_i, x''_i]^\top, i \in \mathcal{I}_m \backslash \mathcal{I}_0.$$

Thus, we can obtain the following system of linear equations with respect to $q_{\mathcal{I}_m}$:

$$-L_m \otimes I_2 \cdot q_{\mathcal{I}_m} = [\overbrace{x_1', x_1'', ..., x_i', x_i''}^{2\cdot|\mathcal{I}_m\backslash\mathcal{I}_0|}, \overbrace{0, ..., 0}^{2\cdot|\mathcal{I}_0|}]^\top. \quad (41)$$

Using $A \cdot q_{\mathcal{I}_m} = B$ as the shorthand for the above system of linear equations. It is observed that for any B with $|\mathcal{I}_0| \geq 1$, there always holds that $\text{rank}(A) = \text{rank}(A, B) = 2 \cdot |\mathcal{I}_m| - 2$ because the first $|\mathcal{I}_m| - 1$ rows of L_m are always linearly independent.

It is worth noting that $\sum_{i\in\mathcal{I}_m} u_{i_m} = 0$ by Lemma 3, which leads to

$$\sum_{i\in\mathcal{I}_m\backslash\mathcal{I}_0} x_i' = 0, \sum_{i\in\mathcal{I}_m\backslash\mathcal{I}_0} x_i'' = 0. \quad (42)$$

Then, substitute (41) in (38), we have

$$\overbrace{[(p_1^*)', (p_1^*)'', ..., (p_i^*)', (p_i^*)'']}^{2\cdot|\mathcal{I}_m\backslash\mathcal{I}_0|} \cdot \overbrace{[x_1'', -x_1', ..., x_i'', -x_i']}^{2\cdot|\mathcal{I}_m\backslash\mathcal{I}_0|}{}^\top = 0, i \in \mathcal{I}_m\backslash\mathcal{I}_0. \quad (43)$$

Substitute (41) in (39), we have

$$\overbrace{[(p_1^*)', (p_1^*)'', ..., (p_i^*)', (p_i^*)'']}^{2\cdot|\mathcal{I}_m\backslash\mathcal{I}_0|} \cdot \overbrace{[x_1', x_1'', ..., x_i', x_i'']}^{2\cdot|\mathcal{I}_m\backslash\mathcal{I}_0|}{}^\top = 0, i \in \mathcal{I}_m\backslash\mathcal{I}_0. \quad (44)$$

In conclusion, E_{m0} can be viewed as the set of p that satisfies equations (41), (42), (43), and (44).

Next we prove sufficiency and necessity, successively.

Sufficiency: When $|\mathcal{I}_0| = |\mathcal{I}_m| - 2$, the set $\mathcal{I}_m\backslash\mathcal{I}_0$ contains two vertices. According to (42), we have

$$x_1' = -x_2', \ x_1'' = -x_2''. \quad (45)$$

Thus, combine (43), (44) and (45), we have the following system of equations

$$\begin{cases} ((p_1^*)' - (p_2^*)')x_1' + ((p_1^*)'' - (p_2^*)'')x_1'' = 0, \\ ((p_2^*)'' - (p_1^*)'')x_1' + ((p_1^*)' - (p_2^*)')x_1'' = 0. \end{cases} \quad (46)$$

Since any two vertices do not coincide in the target formation, i.e., $[(p_1^*)', (p_1^*)'']^\top \neq [(p_2^*)', (p_2^*)'']^\top$, the coefficient matrix of the linear equation always has a nonzero determinant. Therefore, $x_1' = x_1'' = x_2' = x_2'' = 0$, which follows that $E_{m0} \subseteq E_m$.

Necessity: Assume $|\mathcal{I}_0| < |\mathcal{I}_m| - 2$, we consider the case of $|\mathcal{I}_0| = |\mathcal{I}_m| - 3$. The set $\mathcal{I}_m\backslash\mathcal{I}_0$ contains three vertices. Similarly, according to (42), we have

$$x_3' = -x_1' - x_2', \ x_3'' = -x_1'' - x_2''. \quad (47)$$

Combine (43), (44) and (47), we have the following system of equations $A \cdot X = 0$, where

$$A = \begin{bmatrix} (p_1^*)' - (p_3^*)', (p_1^*)'' - (p_3^*)'', (p_2^*)' - (p_3^*)', (p_2^*)'' - (p_3^*)'' \\ (p_3^*)'' - (p_1^*)'', (p_1^*)' - (p_3^*)', (p_3^*)'' - (p_2^*)'', (p_2^*)' - (p_3^*)' \end{bmatrix}, \quad (48)$$

and $X = [x_1', x_1'', x_2', x_2'']^\top$. We can obtain $\text{rank}(A) = 2$, since any two vertices do not coincide. The system of equations has infinitely many solutions. Thus $E_{m0} \nsubseteq E_m$, which is a contradiction. The proof is completed. ■

Lemma 7 implies that the states of $|\mathcal{I}_m| - 2$ agents are sufficient to fix the shape of the whole clique under controller (17). Therefore, similar to [20], one can control the orientation and scale of the whole clique by only controlling two agents in $\mathcal{I}_0$ when $|\mathcal{I}_0| \geq |\mathcal{I}_m| - 2$.

Next we provide an example to illustrate the necessity of Lemma 7 more clearly.

Example 1 *In this example, consider a maxclique containing four vertices, i.e., $|\mathcal{I}_m| = 4$. Fig. 2 shows the desired framework $(\mathcal{G}, p^*)$ and actual framework $(\mathcal{G}, p)$ with the configuration $p = [0, 0, 1.25, 0, 0.75, 0.75, 0, 1.25]^\top$ and $p^* = [0, 0, 1, 0, 1, 1, 0, 1]^\top$, respectively. We can obtain the control input of each agent by (18): $u_1 = [0, 0]^\top, u_2 = [-0.25, 0]^\top, u_3 = [0.25, 0.25]^\top, u_4 = [0, -0.25]^\top$, which indicates $\mathcal{I}_0 = \{1\}$ and $|\mathcal{I}_0| < |\mathcal{I}_m| - 2$. From Fig. 2, we observe that $E_{m0} \nsubseteq E_m$.*

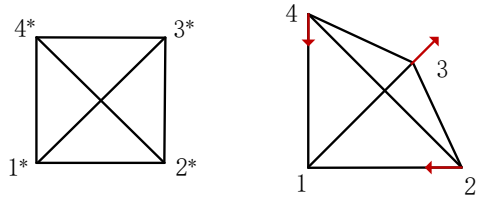

(a) (b)

Fig. 2. The example of Lemma 7. (a) The desired formation. (b) The actual formation. The red arrows represent the directions of control inputs given the desired formation and the actual formation, where the control input of first agent is zero.

Lemma 7 shows that if the number of independent agents of maxclique m satisfies $|\mathcal{I}_0| \geq |\mathcal{I}_m| - 2$, we have $u_{i_m} = 0, i \in \mathcal{I}_m\backslash\mathcal{I}_0$. Based on this idea, together with Assumption 1, Lemma 1 and Lemma 6, it always holds that

$$p \in E^{\{u_i=0\}} \Rightarrow u_{i_m} = 0, m \in \mathcal{M}(\mathcal{G}), i \in \mathcal{I}_m \Rightarrow p \in \mathscr{S},$$

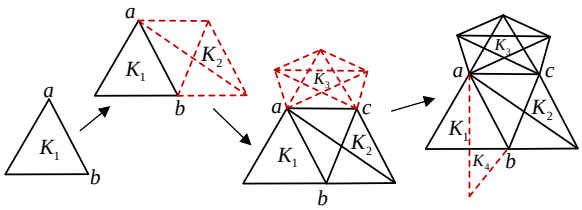

Fig. 3. An example of graph $\mathcal{G}_C$. Starting with the initial clique $K_1 = (\mathcal{V}_1, \mathcal{E}_1)$, we add the new clique $K_2 = (\mathcal{V}_2^c, \mathcal{E}_2^c)$, such that $|\mathcal{V}_1 \cap \mathcal{V}_2^c| = 2$ and $|\mathcal{E}_1 \cap \mathcal{E}_2^c| = 1$. Similarly, we add cliques K_3 and K_4 successively through edges (a, c) and (a, b), respectively, satisfying $|\mathcal{V}_2 \cap \mathcal{V}_3^c| = 2$, $|\mathcal{E}_2 \cap \mathcal{E}_3^c| = 1$, $|\mathcal{V}_3 \cap \mathcal{V}_4^c| = 2$ and $|\mathcal{E}_3 \cap \mathcal{E}_4^c| = 1$.

if the structure of graph $\mathcal{G}$ satisfies a specific condition.

To analyze the equilibrium of the overall formation system, we next introduce a class of graphs that can help establish a connection between clique-wise equilibrium and the overall formation system equilibrium.

4.2 Edge-Based Clique Addition

The following definition gives a specific approach of constructing a desired graph topology.

Definition 1 *(Edge-Based Clique Addition) A graph $\mathcal{G}$ is constructed by edge-based clique addition if it is an element of any sequence of graphs $\{\mathcal{G}(n)\}_{n\geq 1}$ obtained as follows: Start with a clique $\mathcal{G}(1) = (\mathcal{V}_1, \mathcal{E}_1)$ with $|\mathcal{V}_1| \geq 3$, the graph $\mathcal{G}(n)$ is obtained by combining $\mathcal{G}(n-1) = (\mathcal{V}_{n-1}, \mathcal{E}_{n-1})$ with another clique $\mathcal{C}_n = (\mathcal{V}_n^c, \mathcal{E}_n^c)$ with $|\mathcal{V}_n^c| \geq 3$, i.e., $\mathcal{G}_n = (\mathcal{V}_n \cup \mathcal{V}_n^c, \mathcal{E}_n \cup \mathcal{E}_n^c)$, such that $|\mathcal{V}_{n-1} \cap \mathcal{V}_n^c| = 2$, $|\mathcal{E}_{n-1} \cap \mathcal{E}_n^c| = 1$.*

In the rest of the paper, we denote $\mathcal{G}_C$ as the graph included by edge-based clique addition for symbol simplicity. Fig. 3 shows an example of the construction of $\mathcal{G}_C$. In fact, the $\mathcal{G}_C$ has three important properties as follows.

- The 2-*intersection graph* of $\mathcal{G}_C$, i.e., $\Upsilon_2(\mathcal{G}_C)$, is a tree.
- An edge may exist in arbitrary number of maxcliques in $\mathcal{G}_C$.
- Graph $\mathcal{G}_C$ is generically rigid [2].

Note that Definition 1 only constrains the graph topology $\mathcal{G}$, and is independent of the geometric shape. Moreover, the above graph properties are necessary but not sufficient for Definition 1. To better understand Definition 1, we show three counterexamples in Fig. 4.

[2] Rigidity refers to the property that the shape of a framework $(\mathcal{G}, p)$ can be locally determined by inter-node distance constraints. A graph $\mathcal{G}$ is generically rigid if $(\mathcal{G}, p)$ is rigid for almost all configuration $p \in \mathbb{R}^{2N}$. For more details about rigidity and generic rigidity, please refer to [39,40].

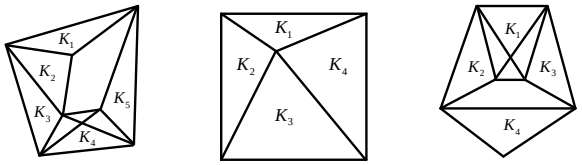

(a) (b) (c)

Fig. 4. Three graphs that are not graph $\mathcal{G}_C$. (a), $|\mathcal{V}_{n-1} \cap \mathcal{V}_n^c| = 3$, $|\mathcal{E}_{n-1} \cap \mathcal{E}_n^c| = 1$. (b), $|\mathcal{V}_{n-1} \cap \mathcal{V}_n^c| = 3$, $|\mathcal{E}_{n-1} \cap \mathcal{E}_n^c| = 2$. (c), $|\mathcal{V}_{n-1} \cap \mathcal{V}_n^c| = 2$, $|\mathcal{E}_{n-1} \cap \mathcal{E}_n^c| = 0$.

Remark 2 *We would like to give the following remarks regarding the proposed "edge-based clique addition" method:*

- *Our condition on graph $\mathcal{G}_C$ is more relaxed compared to the graph condition in [33], as the latter needs to ensure that the common edge of two maxcliques exclusively belong to these two maxcliques.*
- *The rigidity property can be verified by applying successive edge-attachment operations defined in [41].*
- *The triangulated Laman graph, defined in [42], is a special case of graphs constructed by edge-based clique addition.*
- *Although graph $\mathcal{G}_C$ is constructed by a sequence of clique addition, the individual formation controllers (28) are implemented simultaneously.*

4.3 Equilibrium Analysis for the Formation System

Recall the definition of $E^{\{u_i=0\}}$ defined in (30), which is the equilibrium of the formation system. In Remark 1, we claimed that $E^{\{u_i=0\}}$ may not correspond to the desired formation for the whole formation, the following lemma shows that we can establish the equivalence of $E^{\{u_i=0\}}$ and $\mathscr{S}$ provided the graph satisfies Definition 1.

Lemma 8 *$E^{\{u_i=0\}} = \mathscr{S}$ under the graph constructed by edge-based clique addition, i,e, $\mathcal{G}_C$.*

Proof. Define $E^{\{u_{i_m}=0\}} = \{p \in \mathbb{R}^{2N} : u_{i_m} = 0, k_m \in \mathbb{R}^+, R_m(\alpha_m) \in \mathrm{SO}(2), m \in \mathcal{M}(\mathcal{G}), i \in \mathcal{I}_m\}$, which corresponds to the configuration under which each maxclique achieves its desired formation. Next we will prove that

$$E^{\{u_i=0\}} = E^{\{u_{i_m}=0\}} = E^{\{\hat{\gamma}=0\}} = \mathscr{S}$$

under the graph $\mathcal{G}_C$.

Firstly, it is observed that $E^{\{u_{i_m}=0\}} = E^{\{\hat{\gamma}=0\}}$ according to Remark 1 and the expression of $\hat{\gamma}$ in (6). Then, based on the first property of $\mathcal{G}_C$ and Lemma 1, we have $E^{\{\hat{\gamma}=0\}} = \mathscr{S}$.

Next, we prove that $E^{\{u_i=0\}} = E^{\{u_{i_m}=0\}}$. According to the definitions of $E^{\{u_i=0\}}$ and $E^{\{u_{i_m}=0\}}$, we obtain

$E^{\{u_{i_m}=0\}} \subseteq E^{\{u_i=0\}}$ directly. Therefore, it suffices to show $E^{\{u_i=0\}} \subseteq E^{\{u_{i_m}=0\}}$ under graph $\mathcal{G}_C$.

Consider a graph $\mathcal{G}_C$ consisting of $\bar{m}$ maxcliques, we sequentially label the $\bar{m}$ maxcliques by $1, 2, ..., \bar{m}$ based on the construction order of graph $\mathcal{G}_C$. According to the definition of graph $\mathcal{G}_C$, for any maxclique i, it shares only one common edge with maxclique j labeled less than i.

Next we will prove that $u_{i_m} = 0, m \in \mathcal{M}(\mathcal{G}), i \in \mathcal{I}_m$ by the principle of mathematical induction.

For maxclique $\bar{m}$ of graph $\mathcal{G}$, it has only one common edge with other maxcliques, implying $u_{i_{\bar{m}}} = 0, i \in \mathcal{I}_{\bar{m}}$ by Lemma 7.

We assume maxclique $n, n \in \{2, .., \bar{m}\}$ satisfies $u_{i_{\bar{n}}} = 0, i \in \mathcal{I}_n$. Then, consider maxclique $n-1$, it shares one common edge (a, b) with maxcliques labeled less than $n-1$. We can have $u_{i_{n-1}} = 0, i \in \mathcal{I}_{n-1} \backslash \{a, b\}$ regardless of whether maxclique $n-1$ has intersections with maxcliques labeled greater than $n-1$. Therefore, $u_{i_{n-1}} = 0, i \in \mathcal{I}_{n-1}$ according to Lemma 7.

By the principle of mathematical induction, we can obtain $u_{i_m} = 0, m \in \mathcal{M}(\mathcal{G})$ for any $i \in \mathcal{I}_m$, implying $E^{\{u_i=0\}} \subseteq E^{\{u_{i_m}=0\}}$. The proof is completed. ■

Lemma 8 implies that once the graph satisfies Definition 1, the equilibrium of the overall formation system always corresponds to the desired formation shape. Hence, now we can go ahead to provide the stability analysis for the formation equilibrium.

5 Stability Analysis

The following theorem shows the global stability of the desired formation shape via controller (18) and edge-based clique addition.

Theorem 1 *The multi-agent system* (1) *under the control input (18) globally converges to the desired equilibrium set, if the formation graph is constructed by edge-based clique addition.*

Proof. Define a Lyapunov candidate function as

$$V = \hat{\gamma} = \sum_{m \in \mathcal{M}(\mathcal{G}_c)} \gamma_m = \sum_{m \in \mathcal{M}(\mathcal{G}_c)} \left[\sum_{i \in \mathcal{I}_m} \sum_{j \in \mathcal{I}_m} \left\| p_{ij} - k_m R_m p_{ij}^* \right\|^2 \right] \geq 0. \quad (49)$$

The derivation of the Lyapunov function for the single-integrator is obtained as follows:

$$\dot{V} = \sum_{i \in \mathcal{V}} (\nabla_{p_i} V)^\top \dot{p}_i = -\sum_{i \in \mathcal{V}} u_i^\top \dot{p}_i = -\sum_{i \in \mathcal{V}} \|u_i\|^2 \leq 0. \quad (50)$$

According to Lemma 3, it holds that $\|p\| \leq \|p(0)\|$ for all $t \geq 0$. Therefore, we can find a compact set $\Omega = \{p | \|p\| \leq \|p(0)\|\}$. Invoking LaSalle's invariance principle [43], the system converges asymptotically to the largest invariant $E^{\{u_i=0\}}$. Recall Lemma 8, we have $E^{\{u_i=0\}} = \mathscr{S}$. The proof is completed. ■

Theorem 1 establishes the global asymptotic convergence by using LaSalle's invariance principle, which is similar to [32,33]. The main novelty of Theorem 1 is that the graphical condition for the convergence of similar formation is further relaxed as "edge-based clique addition", by virtue of Lemma 8.

6 Simulations

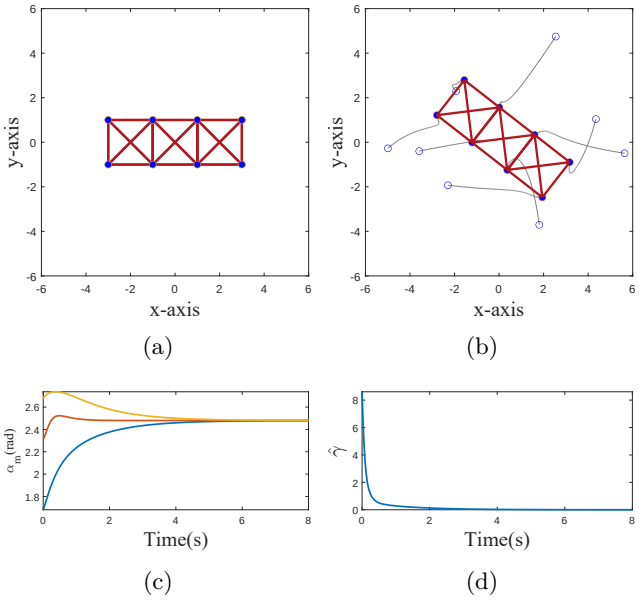

Fig. 5. The simulation results of the control strategy in [33]. (a) The desired framework $(\mathcal{G}, p^*)$. (b) The convergence process of the actual formation. The blue hollow circles and the blue solid circles represent the initial positions and converged positions, respectively. Each solid gray line illustrates the motion trajectory of each agent. (c) The convergence of the rotation angle α_m of each maxclique in the global coordinate frame. (d) The evolution of the cost function $\hat{\gamma}$.

To verify the performance of our proposed similar formation controller via Edge-Based Clique Addition, we conduct comparative experiments with relevant works.

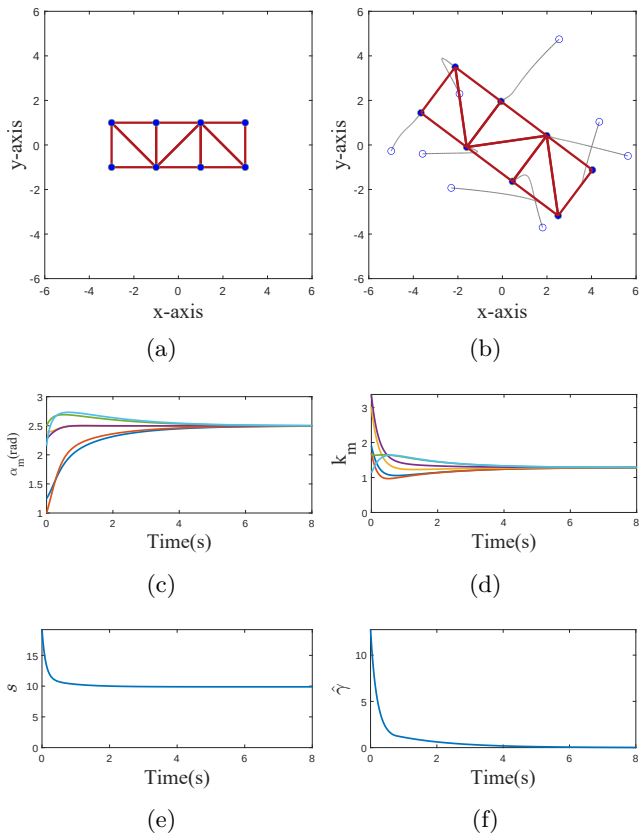

Fig. 6. The simulation results of our proposed control strategy. (a) The desired framework $(\mathcal{G}, p^*)$. (b) The convergence process of the actual formation. (c) The convergence of rotation angle α_m of each maxclique in the global coordinate frame. (d) The convergence of scale parameter k_m of each maxclique. (e) The evolution of the scale s. (f) The evolution of the cost function $\hat{\gamma}$.

In [31,32], the authors proved the global convergence of similar formation under a complete graph. In [33], formation rotation and translation are achieved based on constraints between cliques. Since the condition in the latter is milder than the former, we only compare with [33] to show that our controller requires fewer sensing links when facing the same formation stabilization mission. Moreover, the stabilized formation via our controller is able to have a different scale against the prescribed target formation.

In the comparative simulations, we aim to form a rectangular-shaped formation using eight agents with $p^* = [(p_1^*)^\top, (p_2^*)^\top, ..., (p_N^*)^\top]^\top \in \mathbb{R}^{2N}$, $p_1^* = [-3,-1]^\top, p_2^* = [-1,-1]^\top, p_3^* = [1,-1]^\top, p_4^* = [3,-1]^\top, p_5^* = [3,1]^\top, p_6^* = [1,1]^\top, p_7^* = [-1,1]^\top, p_8^* = [-3,1]^\top$. Each agent i can measure the relative positions of its neighbors in $\mathcal{N}_i$.

According to the graph construction method provided by [33, Lemma 1], we can construct the topology shown in Fig. 5a that the blue solid circles and the red solid lines represent vertices and edges, respectively. This topology contains 3 maxcliques and 16 edges. However, based on the Edge-Based Clique Addition proposed in our paper, we can construct a more relaxed topology structure shown in Fig. 6a, which contains contains 6 maxcliques and 13 edges. The experimental results based on the above different topology structure with their corresponding control strategies are shown as follows.

Both methods use the same random initial positions. Fig. 5b illustrates the convergence process of the actual formation under the control strategy and graph structure in [33]. Fig. 6b shows the convergence process of the actual formation under our proposed control strategy and graph structure, where the multi-agents converge to the desired formation shape up to rotation, translation and scaling. It is observed that compared to [33], our controller renders not only a relaxed graph structure, but also an extra degree of freedom, i.e., formation scaling.

Fig. 6c and Fig. 6d show the evolution of rotations and scaling factors of different maxcliques in the global coordinate frame, respectively. For convenience of illustration, according to Lemma 5, we only focus on the rotation of each maxclique rather than each agent. It is observed that all the rotations and scaling factors converge to a common value asymptotically, respectively. Fig. 6e depicts the variation of the formation scale s, which is non-increasing, as stated in Lemma 3. Fig. 6f illustrates that the global cost $\hat{\gamma}$ decreases as time goes by and converges to zero when the desired formation is achieved. Note that although we did not obtain an analytical expression for the formation convergence rate, it is observed from Fig. 6f that exponential convergence is achieved.

7 Conclusion

In this article, we have presented a distributed similar formation control method based on cliques. The underlying philosophy of the control strategy is to coordinate the rotation matrices and scaling factors of different maxcliques based on the common edges between maxcliques, thereby achieving the overall translation, rotation, and scaling of the formation. We proposed a necessary and sufficient condition for a clique to determine its formation shape when only partial agents are constrained. Based on this condition, we provided a novel graph construction approach termed as "edge-based clique addition". We proved that the multi-agent system under our controller globally converges to the desired equilibrium set if the formation graph is constructed by edge-based clique addition. The proposed approach offers a promising advancement in the field of distributed formation control with practical implications for multi-agent systems. In future, we will explore more relaxed graphical conditions for similar formation control based on local

relative position measurements. In addition, we will try to extend the present work to higher-dimensional spaces.

References

[1] Mohamed A Kamel, Xiang Yu, and Youmin Zhang. Formation control and coordination of multiple unmanned ground vehicles in normal and faulty situations: A review. *Annual reviews in control*, 49:128–144, 2020.

[2] Hanlin Wang and Michael Rubenstein. Shape formation in homogeneous swarms using local task swapping. *IEEE Transactions on Robotics*, 36(3):597–612, 2020.

[3] Guibin Sun, Rui Zhou, Zhao Ma, Yongqi Li, Roderich Groß, Zhang Chen, and Shiyu Zhao. Mean-shift exploration in shape assembly of robot swarms. *Nature Communications*, 14(1):3476, 2023.

[4] Kwang-Kyo Oh, Myoung-Chul Park, and Hyo-Sung Ahn. A survey of multi-agent formation control. *Automatica*, 53:424–440, 2015.

[5] Reza Olfati-Saber, J Alex Fax, and Richard M Murray. Consensus and cooperation in networked multi-agent systems. *Proceedings of the IEEE*, 95(1):215–233, 2007.

[6] J Alexander Fax and Richard M Murray. Information flow and cooperative control of vehicle formations. *IEEE transactions on automatic control*, 49(9):1465–1476, 2004.

[7] Kwang-Kyo Oh and Hyo-Sung Ahn. Formation control and network localization via orientation alignment. *IEEE Transactions on Automatic Control*, 59(2):540–545, 2013.

[8] Dongyu Li, Shuzhi Sam Ge, and Tong Heng Lee. Fixed-time-synchronized consensus control of multiagent systems. *IEEE transactions on control of network systems*, 8(1):89–98, 2020.

[9] Dongyu Li, Shuzhi Sam Ge, Wei He, Guangfu Ma, and Lihua Xie. Multilayer formation control of multi-agent systems. *Automatica*, 109:108558, 2019.

[10] Laura Krick, Mireille E Broucke, and Bruce A Francis. Stabilisation of infinitesimally rigid formations of multi-robot networks. *International Journal of control*, 82(3):423–439, 2009.

[11] Changbin Yu, Brian DO Anderson, Soura Dasgupta, and Barış Fidan. Control of minimally persistent formations in the plane. *SIAM Journal on Control and Optimization*, 48(1):206–233, 2009.

[12] Kwang-Kyo Oh and Hyo-Sung Ahn. Formation control of mobile agents based on inter-agent distance dynamics. *Automatica*, 47(10):2306–2312, 2011.

[13] Zhiyong Sun, Myoung-Chul Park, Brian DO Anderson, and Hyo-Sung Ahn. Distributed stabilization control of rigid formations with prescribed orientation. *Automatica*, 78:250–257, 2017.

[14] Julien M Hendrickx, Brian DO Anderson, Jean-Charles Delvenne, and Vincent D Blondel. Directed graphs for the analysis of rigidity and persistence in autonomous agent systems. *International Journal of Robust and Nonlinear Control: IFAC-Affiliated Journal*, 17(10-11):960–981, 2007.

[15] Tolga Eren. Formation shape control based on bearing rigidity. *International Journal of Control*, 85(9):1361–1379, 2012.

[16] Shiyu Zhao and Daniel Zelazo. Bearing rigidity and almost global bearing-only formation stabilization. *IEEE Transactions on Automatic Control*, 61(5):1255–1268, 2015.

[17] Daniel Zelazo, Paolo Robuffo Giordano, and Antonio Franchi. Bearing-only formation control using an se (2) rigidity theory. In *2015 54th ieee conference on decision and control (cdc)*, pages 6121–6126. IEEE, 2015.

[18] Shiyu Zhao and Daniel Zelazo. Translational and scaling formation maneuver control via a bearing-based approach. *IEEE Transactions on Control of Network Systems*, 4(3):429–438, 2015.

[19] Xu Fang, Jitao Li, Xiaolei Li, and Lihua Xie. 2-d distributed pose estimation of multi-agent systems using bearing measurements. *Journal of Automation and Intelligence*, 2(2):70–78, 2023.

[20] Gangshan Jing, Guofeng Zhang, Heung Wing Joseph Lee, and Long Wang. Angle-based shape determination theory of planar graphs with application to formation stabilization. *Automatica*, 105:117–129, 2019.

[21] Liangming Chen, Ming Cao, and Chuanjiang Li. Angle rigidity and its usage to stabilize multiagent formations in 2-d. *IEEE Transactions on Automatic Control*, 66(8):3667–3681, 2020.

[22] Ian Buckley and Magnus Egerstedt. Infinitesimal shape-similarity for characterization and control of bearing-only multirobot formations. *IEEE Transactions on Robotics*, 37(6):1921–1935, 2021.

[23] Wei Ren and Ella Atkins. Distributed multi-vehicle coordinated control via local information exchange. *International Journal of Robust and Nonlinear Control: IFAC-Affiliated Journal*, 17(10-11):1002–1033, 2007.

[24] Gangshan Jing, Guofeng Zhang, Heung Wing Joseph Lee, and Long Wang. Weak rigidity theory and its application to formation stabilization. *SIAM Journal on Control and optimization*, 56(3):2248–2273, 2018.

[25] Liangming Chen and Zhiyong Sun. Globally stabilizing triangularly angle rigid formations. *IEEE Transactions on Automatic Control*, 68(2):1169–1175, 2022.

[26] Zhiyun Lin, Lili Wang, Zhimin Han, and Minyue Fu. Distributed formation control of multi-agent systems using complex laplacian. *IEEE Transactions on Automatic Control*, 59(7):1765–1777, 2014.

[27] Xu Fang, Lihua Xie, and Xiaolei Li. Distributed localization in dynamic networks via complex laplacian. *Automatica*, 151:110915, 2023.

[28] Zhiyun Lin, Lili Wang, Zhiyong Chen, Minyue Fu, and Zhimin Han. Necessary and sufficient graphical conditions for affine formation control. *IEEE Transactions on Automatic Control*, 61(10):2877–2891, 2015.

[29] Shiyu Zhao. Affine formation maneuver control of multiagent systems. *IEEE Transactions on Automatic Control*, 63(12):4140–4155, 2018.

[30] Kun Li, Zhixi Shen, Gangshan Jing, and Yongduan Song. Angle-constrained formation control under directed non-triangulated sensing graphs. *Automatica*, 163:111565, 2024.

[31] Kazunori Sakurama, Shun-Ichi Azuma, and Toshiharu Sugie. Multiagent coordination via distributed pattern matching. *IEEE Transactions on Automatic Control*, 64(8):3210–3225, 2018.

[32] Kazunori Sakurama. Unified formulation of multiagent coordination with relative measurements. *IEEE Transactions on Automatic Control*, 66(9):4101–4116, 2020.

[33] Miguel Aranda, Gonzalo Lopez-Nicolas, Carlos Sagüés, and Michael M Zavlanos. Distributed formation stabilization using relative position measurements in local coordinates. *IEEE Transactions on Automatic Control*, 61(12):3925–3935, 2016.

[34] Béla Bollobás. *Modern graph theory*, volume 184. Springer Science & Business Media, 1998.

[35] Terry A McKee and Fred R McMorris. *Topics in intersection graph theory*. SIAM, 1999.

[36] Shiyu Zhao and Zhiyong Sun. Defend the practicality of single-integrator models in multi-robot coordination control. In *2017 13th IEEE International Conference on Control & Automation (ICCA)*, pages 666–671. IEEE, 2017.

[37] Brian DO Anderson, Changbin Yu, Baris Fidan, and Julien M Hendrickx. Rigid graph control architectures for autonomous formations. *IEEE Control Systems Magazine*, 28(6):48–63, 2008.

[38] Gene H Golub and Charles F Van Loan. *Matrix computations*. JHU press, 2013.

[39] Leonard Asimow and Ben Roth. The rigidity of graphs, ii. *Journal of Mathematical Analysis and Applications*, 68(1):171–190, 1979.

[40] Robert Connelly. Generic global rigidity. *Discrete & Computational Geometry*, 33:549–563, 2005.

[41] Reza Olfati-Saber and Richard M Murray. Graph rigidity and distributed formation stabilization of multi-vehicle systems. In *Proceedings of the 41st IEEE Conference on Decision and Control, 2002.*, volume 3, pages 2965–2971. IEEE, 2002.

[42] Xudong Chen, Mohamed-Ali Belabbas, and Tamer Başar. Global stabilization of triangulated formations. *SIAM Journal on Control and Optimization*, 55(1):172–199, 2017.

[43] Hassan K Khalil. *Nonlinear systems*. Prentice Hall, New York, NY, 2002.

He Gen received the B.E. degree in automation from Southwest Petroleum University, China, in 2022. He is currently working toward a master's degree at the College of Automation, Chongqing University. His research interests include rigidity theory, formation control, and multi-agent systems.

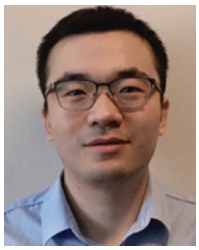

Gangshan Jing received the Ph.D. degree in control theory and control engineering from Xidian University, Xi'an, China, in 2018. From 2016 to 2017, he was a Research Assistant with Hong Kong Polytechnic University, Hong Kong. From 2018 to 2021, he was a Postdoctoral Researcher with Ohio State University, Columbus, OH, USA, and North Carolina State University, Rayleigh, NC, USA, respectively. Since 2021, he has been a Faculty Member with Chongqing University, Chongqing, China. His research interests include control, optimization, and machine learning for network system.

YongDuan Song is a Fellow of IEEE, Fellow of AAIA, Fellow of International Eurasian Academy of Sciences, and Fellow of Chinese Automation Association. He was one of the six Langley Distinguished Professors at National Institute of Aerospace (NIA), USA and register professional engineer (USA). He is currently the dean of Research Institute of Artificial Intelligence at Chongqing University. Professor Song is the Editor-in-Chief of IEEE Transactions on Neural Networks and Learning Systems (TNNLS) and the founding Editor-in-Chief of the International Journal of Automation and Intelligence. His current research interests include intelligent systems, guidance navigation and control, bio-inspired adaptive and cooperative systems.